ICES Journal of Marine Science Advance Access published April 7, 2016

ICES Journal of Marine Science

ICES Journal of Marine Science; doi:10.1093/icesjms/fsw040

Modelling spatially dependent predation mortality of eastern Bering Sea walleye pollock, and its implications for stock dynamics under future climate scenarios

Paul D. Spencer[1]*, Kirstin K. Holsman[1], Stephani Zador[1], Nicholas A. Bond[2], Franz J. Mueter[3], Anne B. Hollowed[1], and James N. Ianelli[1]

[1]*NOAA-Fisheries, Alaska Fisheries Science Center, Seattle, WA, USA*
[2]*Joint Institute for the Study of Atmosphere and Ocean (JISAO), Seattle, WA, USA*
[3]*Juneau Center, School of Fisheries and Ocean Sciences, University of Alaska Fairbanks, Juneau, AK, USA*

**Corresponding author: tel +1 206 526 4248; fax +1 206 526 6723; e-mail: paul.spencer@noaa.gov*

Spencer, P. D., Holsman, K. K., Zador, S., Bond, N. A., Mueter, F. J., Hollowed, Anne B., and Ianelli, J. N. Modelling spatially dependent predation mortality of eastern Bering Sea walleye pollock, and its implications for stock dynamics under future climate scenarios. – ICES Journal of Marine Science, doi: 10.1093/icesjms/fsw040.

Received 31 May 2015; revised 28 January 2016; accepted 3 February 2016.

Arrowtooth flounder (*Atheresthes stomias*) are an important predator of juvenile walleye pollock (*Gadus chalcogramus*) in the eastern Bering Sea (EBS) shelf and have increased 3-fold in biomass from 1977 to 2014. Arrowtooth flounder avoid the summer "cold pool" (bottom water $\leq 2^{\circ}$C) and variability in cold pool size and location has affected their spatial overlap with juvenile walleye pollock. Developing a method to account for the relationship between climate change and pollock mortality can highlight ecosystem dynamics and contribute to better assessments for fisheries management. Consequently, spatially resolved predation mortality rates were estimated within an age-structured walleye pollock stock assessment population model (based on spatial information on diet and abundance from trawl surveys), along with the effect of sea surface temperature (SST) on pollock recruitment. Projections of SST and cold pool area to 2050 were obtained (or statistically downscaled) from nine global climate models and used within an age-structure population model to project pollock abundance given estimated relationships between environmental variables and predator and prey spatial distributions, pollock recruitment, and maximum rate of arrowtooth flounder consumption. The climate projections show a wide range of variability but an overall trend of increasing SST and decreasing cold pool area. Projected pollock biomass decreased largely due to the negative effect of increased SST on pollock recruitment. A sensitivity analysis indicated that the decline in projected pollock biomass would be exacerbated if arrowtooth flounder increased their relative distribution in the EBS northwest middle shelf (an area of relatively high density of juvenile pollock) in warm years.

Keywords: arrowtooth flounder, Bering Sea, climate change, forecasting, functional response, predation, recruitment, spatial overlap, statistical downscaling, walleye pollock.

Introduction

Ocean temperatures have been increasing, with the rates of increase since the early 1970s being highest in the upper 75 m (Hoegh-Guldberg *et al.*, 2014) and thereby influencing biologically productive continental shelf ecosystems. Increased temperatures can affect the productivity and population dynamics of fish stocks via myriad mechanisms, including direct effects on the behaviour and physiology of individual organisms, or indirect effects on ecosystem structure (Brander, 2007). Examples of direct effects of climate change include changes in spatial distributions (Mueter and Litzow, 2008; Pinsky *et al.*, 2013) and metabolic rates of consumption and growth (Holsman and Aydin, 2015), whereas indirect effects include the influence of climate change on the abundance and timing of plankton blooms and its result on fish recruitment (Mueter *et al.*, 2011). A challenge for projecting future levels of fish productivity is distinguishing between

these various mechanisms and how they are affected by climate change.

The effect of ocean warming on species distributions has received considerable attention, with many species shifting poleward and/or to deeper waters (Dulvy *et al.*, 2008; Nye *et al.*, 2009). Yet species also exhibit differential responses to changing conditions (i.e. rate and direction of movement), which may be related to biological characteristics (Murawski, 1993; Perry *et al.*, 2005) and the variation of climate velocities (the rate of movement of isotherms; Loarie *et al.*, 2009) in the habitats occupied by fish (Pinsky *et al.*, 2013). Divergent distributional responses to warming can affect predator–prey interactions, as the predator–prey spatial overlap under future climatic conditions is a function of the projected stock distributions among finer-scale subareas. For example, Hunsicker *et al.* (2013) found that the estimated overlap between arrowtooth flounder (*Atheresthes stomias*, an important predator) and juvenile walleye pollock (*Gadus chalcogramus*; hereafter referred to as pollock) on the eastern Bering Sea (EBS) shelf increased with arrowtooth flounder abundance and temperature, and decreased with pollock abundance. The predation impact of EBS arrowtooth flounder on juvenile pollock is currently highest in the northwest (NW) portion of the EBS shelf (Zador *et al.*, 2011).

Temperature also directly affects fish metabolic rates, as the maximum rate of consumption (C_{max}; the weight of consumed prey per predator weight per day) generally increases for a broad range of temperatures before declining sharply as temperature approaches the upper thermal limit. Bioenergetic models that account for the effects of temperature on fish metabolism (Hanson *et al.*, 1997) can be used to estimate daily rations, an important input to multispecies models, and to evaluate how climate change affects foraging and consumption (Rose *et al.* 2008). For example, Holsman and Aydin (2015) estimated that a 2°C increase in water temperature would increase the daily ration of EBS pollock and Pacific cod (*Gadus macrocephalus*), but decrease daily ration and relative foraging rate (i.e. the ratio of daily ration to maximum consumption rate) of EBS arrowtooth flounder.

In contrast to the direct effects considered above, the effect of temperature on prerecruit survival can be considered an indirect effect that may reflect ocean productivity and the abundance of prey. In the EBS, the Oscillating Control Hypothesis (Hunt *et al.*, 2002) predicts that warm years with early ice retreat would be associated with warm temperatures in late spring, rapid zooplankton growth, and increased prey for piscivorous fish; conversely, late ice retreats may provide increased prey for benthic-feeding fish. However, for EBS pollock, unusually warm conditions may decrease prerecruit survival due to a lack of important large zooplankton in the late summer and autumn (Hunt *et al.*, 2008, 2011; Heintz *et al.*, 2013). Mueter *et al.* (2011) applied a modified Ricker stock–recruitment model to estimates of recruits and abundance from the 2009 walleye pollock stock assessment model (Ianelli *et al.*, 2009) to find that prerecruit survival decreases when late summer sea surface temperature (SST) is above ~9°C.

EBS pollock provide a good case study for attempting to develop stock projection models that incorporate various mechanisms by which environmental conditions can affect population dynamics, as the EBS shelf is well studied with good research surveys and many process-oriented studies (Lomas and Stabeno, 2014). The EBS fish community has exhibited a shift northward from 1982 to 2006 (Mueter and Litzow, 2008), although more recent cold years (i.e. from 2006 to 2010) have resulted in southward movement (Kotwicki and Lauth, 2013). Changes in dynamic physical variables such as stratification and temperature can affect EBS species distributions and ecoregion boundaries (Baker and Hollowed, 2014). These studies have not distinguished between different sizes of pollock, but this becomes important when considering how the overlap of pollock prey and their predators may be affected by environmental variability. For example, Hollowed *et al.* (2012) found that age-1 pollock could tolerate a wide range of temperatures, and Hunsicker *et al.* (2013) found that juvenile pollock spatial distributions are less sensitive to temperature than those of arrowtooth flounder. An environmental feature of the EBS shelf is the cold pool, a layer of bottom water <2°C (Wyllie-Echeverria and Wooster, 1998) that is formed from sea ice melt and spring-summer stratification of the middle shelf (Stabeno *et al.*, 2001) (Figure 1). Arrowtooth flounder have been observed to avoid the cold pool (Spencer, 2008).

Projections of the effect of climate change on pollock abundance and productivity can be improved by accounting for the effects on recruitment, predator consumption rates, and predator–prey spatial overlap. Previous analyses have typically emphasized a particular mechanism, focusing on predator consumption (Holsman and Aydin, 2015), predator–prey overlap (Hunsicker *et al.*, 2013), or recruitment (Ianelli *et al.*, 2011; Mueter *et al.*, 2011), but have not addressed how pollock dynamics would be influenced by spatially variable predation rates that may arise from the effect of climate change on predator–prey overlap. Because the processes identified above can be categorized as affecting either prerecruit mortality or predation mortality on recruited fish (defined as fish age 1 and older; Ianelli *et al.*, 2014), the mortality parameters are amenable for estimation in integrated stock assessment models that provide statistical fits to several types of data (Maunder and Punt, 2013). Predation mortality was estimated in the Gulf of Alaska pollock stock assessment model (Hollowed *et al.*, 2000), allowing for an evaluation of the statistical fit to the estimates of predator consumption relative to other input data.

The purpose of this study is to evaluate the relative importance of environmentally driven changes in recruitment, arrowtooth flounder maximum consumption rate, and the spatial overlap between arrowtooth flounder and pollock on the projected dynamics of pollock. First, relationships between bottom temperatures and spatial distributions for arrowtooth flounder and juvenile pollock are assessed. Second, the single-species pollock assessment model (Ianelli *et al.*, 2014) is modified to estimate the effect of temperature on recruitment and spatially explicit predation mortality rates. Finally, a series of projections are conducted to evaluate pollock catch and abundance under projected future levels of the cold pool and SST. Of particular interest is an assessment of how pollock dynamics would be affected if arrowtooth flounder moved farther north as the temperature increased.

Methods

Spatial information on temperature and the densities of pollock and arrowtooth flounder were obtained from the Alaska Fisheries Science Center's annual EBS shelf summer trawl survey (Lauth and Conner, 2014). The survey has been conducted with consistent sampling methodology since 1982, and the survey strata which have been consistently sampled since 1982 are shown in Figure 1. The 50, 100, and 200 m isobaths form the boundaries of the strata comprising the inner shelf (strata 10 and 20), middle shelf (strata 31, 32, 41, 42, and 43), and outer shelf (strata 50, 61, and 62), which are further organized into NW strata (strata 20, 41, 42, 43, 61, and 62) and southeast (SE) strata (strata 10, 31, 32, and 50). Approximately

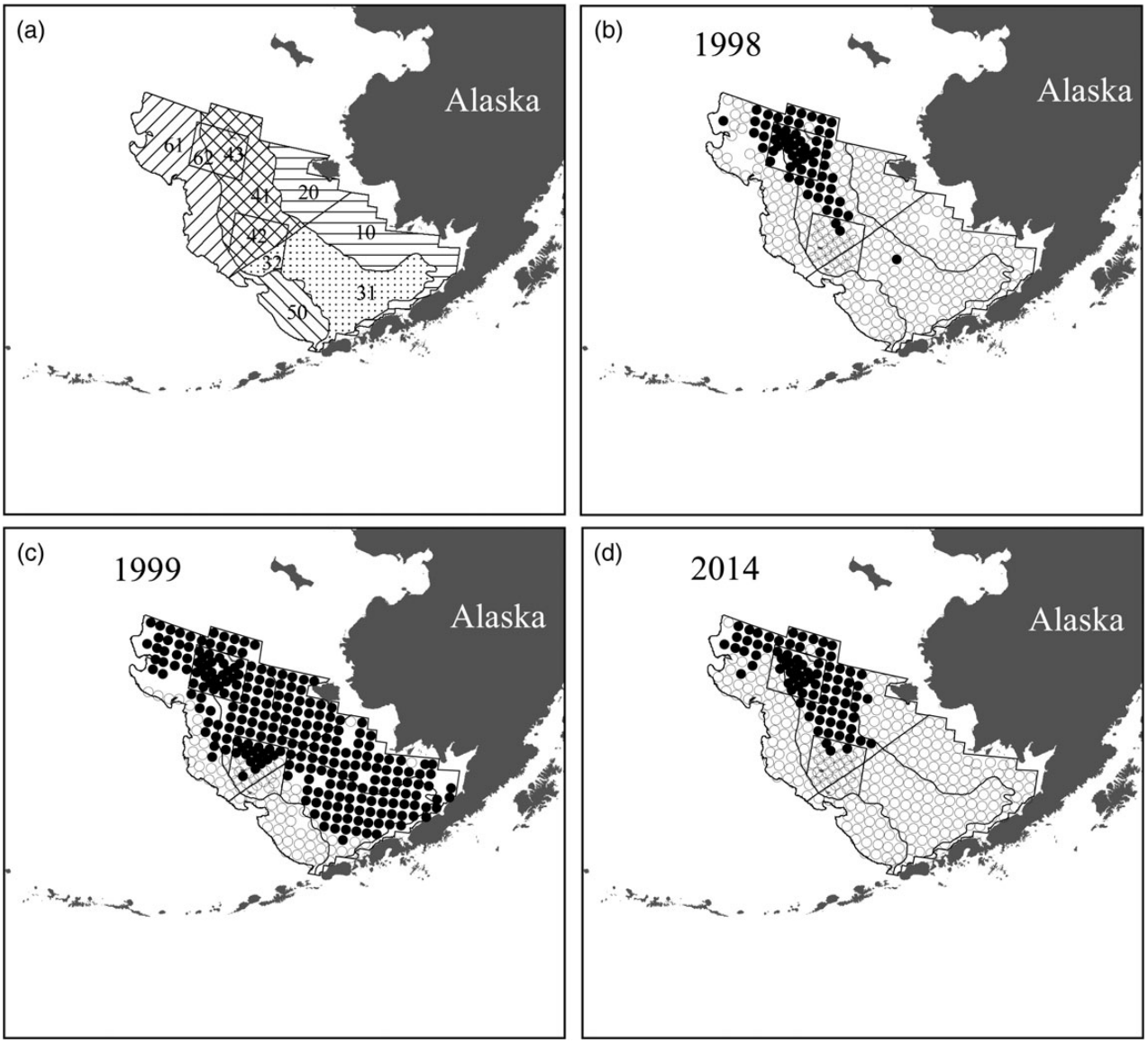

Figure 1. (a) The EBS shelf and strata sampled by bottom trawl survey, with the fill markings distinguishing the five areas defined in Table 1. (b) – (d) The sampling stations, with stations within the cold pool shown in black for cold (1999) and warm (1998, 2014) years.

356 stations located on systematic grid are sampled annually during spring and summer (May to August), with the number and weight of various groundfish species, and bottom temperature, recorded for each station. Arrowtooth flounder stomach weights were opportunistically sampled from the survey catch, and the length and weights of fish prey were obtained from a subset of the non-empty arrowtooth flounder stomach samples. The number of arrowtooth stomachs sampled from 1983 to 2014 by EBS subareas are presented in Table 1.

Influence of temperature on fish distributions

Environmental variability on the EBS shelf is described by the size of the cold pool and the distribution of bottom temperatures. The cold pool area for each year was computed as the total area for survey stations with bottom temperatures $\leq 2^{\circ}$C, where the area for each survey station was defined as the area of the stratum in which it occurs divided by the number of stratum hauls (Perry and Smith, 1994; Spencer, 2008).

The influence of environmental variability on arrowtooth flounder and juvenile pollock distributions (10–20 cm, approximately age 1) was evaluated from the area occupied and catch-weighted temperature distribution for the stock, and the relative distribution of the stock across the EBS shelf. Cumulative frequency distributions (CDFs) were used to estimate the minimum area covered by 95% of the stock by year (Swain and Sinclair, 1994; Spencer, 2008), which was computed as the area represented by survey stations for which the cumulative catch per unit effort (cpue; numbers km^{-2}) was 95% of the cumulative cpue for all stations. Temperature preferences of fish were evaluated with catch-weighted CDFs that indicate temperatures in areas occupied by fish (Perry and Smith, 1994; Spencer, 2008):

$$g(t) = \sum_{i=1}^{h} \sum_{j=1}^{n_i} \frac{w_i}{n_i} \frac{y_{ji}}{\bar{Y}} I(x_{ji}) \text{ where } I(x_{ji}) = \left\{ \begin{array}{ll} 1, & if\ x_{ji} \leq t \\ 0, & \text{otherwise} \end{array} \right\}, \quad (1)$$

Table 1. Number of arrowtooth flounder stomachs sampled for prey composition and prey length from 1983 to 2014, by EBS subarea and arrowtooth flounder size.

		Small ATF (<40 cm)			Large ATF (≥40 cm)		
Area	**Strata**	**Empty**	**Non-empty**	**Sampled for prey lengths**	**Empty**	**Non-empty**	**Sampled for prey lengths**
Inner shelf	10, 20	25	116	11	22	37	3
SE middle shelf	31, 32	861	1029	101	734	696	154
NW middle shelf	41, 42, 43	337	732	136	178	343	123
SE outer shelf	50	816	1069	87	754	680	98
NW middle shelf	61, 62	435	1248	201	946	2282	716

where h is the number of strata, w_i and n_i are the proportion of the survey area and number of hauls, respectively, in stratum i, y_{ij} and x_{ji} are the cpue and bottom temperature, respectively, for haul j and stratum i, $\bar{Y}$ is the stratified mean cpue for the survey, and t spans the range of observed temperatures. The catch-weighted CDFs of temperature were compared with the unweighted CDFs that indicate the temperatures for all areas covered by the survey:

$$f(t) = \sum_{i=1}^{h} \sum_{j=1}^{n_i} \frac{w_i}{n_i} I(x_{ji}) \text{ where } I(x_{ji}) = \left\{ \begin{array}{ll} 1, & \text{if } x_{ji} \le t \\ 0, & \text{otherwise} \end{array} \right\}. \quad (2)$$

The proportions of arrowtooth flounder in two size classes (<40 and ≥40 cm) and juvenile age classes of pollock (ages 1–3) within EBS subareas for each year were estimated from the spatial distribution of survey cpue and were modelled as a function of cold pool area using multinomial logistic regressions, an extension of logistic regression that allows for more than two response categories (Hosmer and Lemeshow, 2000). Limited numbers of tows with positive catch in some strata motivated combining the 10 strata into 5 subareas, as defined in Table 1. Age–length keys from survey sampling were used to convert pollock length compositions within subareas to age compositions. The modelling of spatial distributions as a function of cold pool area allows projections of how future environmental conditions may affect spatial overlap and predation mortality.

Estimation of temperature-dependent recruitment and predation mortality in the pollock stock assessment model

The EBS walleye pollock stock assessment model (Ianelli *et al.*, 2014) was modified to estimate the effect of temperature on recruitment and predation mortality. The Ricker stock–recruitment (Ricker, 1975) curve was used to model age-1 recruitment, and the residuals ε_{SR} between the estimated recruitment and the predicted values from the Ricker curve were modelled as a quadratic function of SST in the year of spawning:

$$\varepsilon_{SR,t+1} = \theta_0 + \theta_1 SST_t + \theta_2 SST_t^2 + \varepsilon_{SST,t+1}, \quad (3)$$

where SST is an index of late summer (July–September) temperatures in year t. The SST index was derived from monthly extended reconstructed SSTs (Smith *et al.*, 2008), from which interpolated values over a $2^\circ \times 2^\circ$ grid covering the Bering Sea shelf were averaged from July through September (Mueter *et al.*, 2011). The parameters θ_0, θ_1, and θ_2 were obtained by minimizing the sum of squares of the residuals ε_{SST} as part of the assessment model objective function.

Temperature can affect predation mortality rates through temperature-dependent changes in spatial distributions and predator–prey overlap. Predation mortality rates can be estimated in stock assessment models in a manner analogous to estimation of fishing morality rates (Hollowed *et al.*, 2000). Given survey data on predator and prey distributions described above, this approach can be extended to estimate spatially explicit predation mortality rates and further requires estimates of predator abundance and prey consumption by age class. Modelling of the predation mortality on pollock ages 1–3 for the two size classes of arrowtooth flounder (<40 and ≥40 cm) was motivated by changes in the proportion of pollock in the diet with arrowtooth flounder size (Zador *et al.*, 2011).

Shelf-wide consumption, by year, of pollock age class (a) by arrowtooth size class (s) was estimated as

$$C_{a,s} = \left(\frac{Q}{B}\right) \bar{B}_s p_a, \quad (4)$$

where (Q/B) is an annual consumption to biomass ratio, $\bar{B}_s$ is the estimated mean biomass within a year of arrowtooth founder for size class s, and p_a is the proportion (by weight) of pollock of age a in the diet. Holsman and Aydin (2015) evaluated a variety of field- and model-based methods for estimating consumption rates of Alaska groundfish, and obtained Q/B ratios of 3.11 and 2.26 for arrowtooth flounder larger and smaller than 40 cm, respectively, from application of a generalized von Bertalanffy growth equation (Essington *et al.*, 2001). Yearly mean biomass for the two size classes of arrowtooth flounder were computed from stock assessment estimates of abundance (Spies *et al.*, 2014).

Yearly estimates of p_a that account for spatial patterns in consumption were generated. For each subarea and year, the proportion (by weight) of pollock by age in the diet of arrowtooth flounder was calculated as the product of the proportion of pollock in the diet (obtained from the non-empty stomachs) and estimated age composition of consumed pollock. Estimated age composition (by weight) of consumed pollock was calculated by applying age–length keys (obtained from survey sampling) to the prey length composition (obtained from stomach sampling) and using mean weight of pollock at age in the stock (Ianelli *et al.*, 2014) to convert to age composition by weight. Shelf-wide estimates of age composition of pollock in the diet for each year were obtained from an average of the subarea values, weighted by the survey cpue of arrowtooth flounder in each subarea. Estimates of the proportion of pollock in the diet, and age composition of the pollock prey, for subareas with low sample sizes (i.e. ≤4) were set to yearly shelf-wide estimates.

Given estimates of consumption described above, predation mortality was estimated within the assessment model with a Holling type II functional response. For each year, the estimated consumption ($\hat{C}_{s,a,h}$) of pollock of age a by arrowtooth flounder

of size class s in subarea h was modelled as

$$\hat{C}_{s,a,h} = \left(\frac{m_{atf,s}}{m_{p,a}} \frac{C_{\max,s,h}\alpha_{a,s}}{\beta_{a,s} + \bar{N}_{a,h}}\right) \bar{E}_{s,h} \bar{N}_{a,h} A_h, \quad (5)$$

where $C_{max,s,h}$ is the maximum rate of consumption for arrowtooth flounder of size class s (in units of grams consumption per gram of predator per year) in subarea h, $\alpha_{a,s}$, and $\beta_{a,s}$ are parameters of a type II functional response curve for pollock age a and arrowtooth size class s, $\bar{N}_{a,h}$ is the mean pollock density of age a in subarea h within the year (accounting for all mortality sources), $\bar{E}_{s,h}$ is the mean arrowtooth flounder abundance of size class s in subarea h within the year, and A_h is the area (km^2) of subarea h. The weights of arrowtooth flounder of size class s and pollock of size a ($m_{atf,s}$ and $m_{p,a}$, respectively) are required to convert the consumption to units of numbers consumed per predator.

The maximum rate of consumption is a function of temperature and fish size:

$$C_{\max,s} = d * C_A W^{C_B} * f(T), \quad (6)$$

where d is the number of feeding days within a year (365 for arrowtooth flounder; Holsman and Aydin, 2015), C_A and C_B are parameters of an allometric consumption equation, and $f(T)$ is a multiplicative scaling function. Estimates of $C_{max,s,h}$ per year were obtained outside the assessment model from the arrowtooth flounder maximum consumption equation presented in Holsman and Aydin (2015), the estimated size of arrowtooth flounder in each size class (calculated from the estimated numbers at age; Spies *et al.*, 2014), and the bottom temperatures by subarea. Over the range of bottom temperatures observed on the EBS shelf, increases in temperatures would increase the rate of maximum consumption (Supplementary Figure S1).

The term within the parentheses in Eq. 5 is a catchability coefficient that models the proportion of the stock removed per year by a unit of effort (in this case, the proportion of pollock removed by a unit of arrowtooth flounder abundance). Equation 5 is analogous to the Baranov catch equation of $C = qE\bar{N}$ with two important differences: (i) the catchability coefficient, q, is modelled as a function of prey density; and (ii) the spatial overlap between predators and prey is incorporated by considering their densities within each subarea. The observed spatial distributions of pollock and arrowtooth flounder from the survey cpue data (described above) were used to partition the modelled pollock abundance and estimated arrowtooth flounder abundance from stock assessments (Spies *et al.*, 2014) across the subareas for each year.

The total natural mortality for pollock of age a (M_a) is the sum of arrowtooth flounder predation mortality and residual mortality

$$M_a = M_{a,resid} + \sum_s M_{a,s}, \quad (7)$$

where the residual mortality $M_{a,resid}$ accounts for all other mortality sources other than the two arrowtooth flounder size classes in the summation term. The current pollock stock assessment fixes M at 0.9, 0.45, and 0.3 for ages 1,2, and 3+, respectively, and these values are consistent with estimates of natural mortality derived from relationships with fish size (Ianelli *et al.*, 2014). To facilitate parameter estimation and scale population abundances to relatively similar levels as those currently estimated, the total M_a from equation (7) were estimated with Bayesian prior distributions, with coefficients of variation (CV) of 0.1 and the distribution means set to the fixed values of M_a from the stock assessment.

Estimated values of $\alpha_{a,s}$ and $\beta_{a,s}$ were obtained by including in the model likelihood function the residuals between estimated and observed total consumption of pollock of ages 1–3, and the residuals in the age composition of consumed pollock. Distribution functions with relatively high levels of variability were used to fit the estimated consumption, reflecting the uncertainty in the diet data and consumption estimates. A lognormal distribution with a CV of 0.7 was used to model the residuals for total consumption, whereas a multinomial distribution with a sample size of 50 was used to model the age composition of pollock consumed by arrowtooth flounder.

Projections of the effects of future climatic conditions on pollock recruitment and arrowtooth flounder predation

The estimated relationships between environmental conditions and recruitment, spatial distributions, and predation mortality were used in a population dynamics model to project the estimated abundance and catch of pollock accounting for variability in recruitment and future climate conditions. A Tier 3 harvest control that reduces fishing mortality at low stock sizes (NPFMC, 2014) was used, but the total catch was limited to 1.5×10^6 t because pollock catches would not be expected to exceed this amount under the 2.0×10^6 t limit for the sum of all Bering Sea/Aleutian Islands groundfish catches. Predation mortality is a function of future abundance of arrowtooth flounder, which was projected from the current estimated numbers at age (Spies *et al.*, 2014) with fishing mortality set to the average of estimates for 2009–2014 and future recruitment set to the average of the estimated recruitment for the 1977–2014 year classes. Each set of projections consisted of 1000 model runs that projected the stock dynamics from 2014 to 2050.

Sensitivity analyses were conducted to evaluate to the role of environmental variability on either recruitment (dependent on SST), maximum consumption rate (dependent on bottom temperatures), and spatial distributions (dependent on cold pool area) on projected abundance and catch of pollock. Separate runs were conducted in which only one of these mechanisms was influenced by projected environmental variability, with the other mechanisms using the historical average of its respective environmental variable.

A sensitivity analysis was also conducted in which arrowtooth flounder moved slightly farther north than would be projected from the estimated relationships between their spatial distribution and the cold pool, and was motivated by the uncertainty in how these relationships would be affected by climate change. This projection was achieved by adjusting the parameters of the multinomial logistic model such that the predicted proportion of small and large arrowtooth flounder in the NW middle shelf was increased to 24 and 22%, respectively, for the year with the smallest observed cold pool; these values were chosen to produce a rate of northward movement (degrees latitude per year) over the projection that is consistent with rates observed in other regions (Pinsky *et al.*, 2013).

Projections of SST were obtained directly from a set of nine global climate model (GCM) simulations carried out on behalf of the Intergovernmental Panel on Climate Change (IPCC) Fifth Assessment Report(AR5; Stocker *et al.*, 2013), whereas cold pool area and bottom temperatures were obtained from statistical downscaling of GCM output. IPCC class GCMs, as a group, are not well suited for specifying summer bottom temperatures in the EBS due to errors associated with improper handling of the bathymetry, tides, and mixing processes near the seabed. Analysis of the historical record indicates that the area and southward extent of the

cold pool corresponds closely with two parameters that can be simulated by GCMs, the maximum sea-ice extent the previous winter, and to a lesser extent, the sea level pressure in spring. A generalized additive model (GAM) based on these two predictors explained 71% of the variance in cold pool extent for 1982–2013. This model was then employed using projections of ice extent and sea level pressure from a set of GCMs with good track records for the Bering Sea (Overland and Wang, 2007). For each stock projection model run, the projected future environmental conditions were obtained from randomly selecting one of the nine climate model simulations. Finally, projections of bottom temperatures by EBS subarea were obtained by applying linear relationships between observed cold pool area and subarea bottom temperatures to the projected estimates of cold pool area.

Results

The area occupied by arrowtooth flounder decreases with the area of the cold pool (Figure 2a). During the three unusually warm years from 2003 to 2005, the area of the cold pool was among its lowest values since 1982 (averaging 57,000 km^2) and the area occupied by arrowtooth flounder were at their highest values and averaged 204,000 km^2. In 1999, the cold pool area was at its largest value and the area occupied by arrowtooth flounder among its lowest values. In contrast, the area occupied by juvenile pollock (10–20 cm) is insensitive to the area of the cold pool.

Catch-weighted temperatures also reveal that arrowtooth flounder avoid the cold pool, even in years when the cold pool is relatively large. Catch-weighted species temperatures are plotted against habitat temperatures in Figure 2b and d for the tenth and 90th percentiles of the frequency distributions (the ○ and + symbols, respectively), and the extent to which the scatterplots deviate from the 1:1 line indicates temperature selection. The tenth percentile of temperature in the EBS shelf is typically <2°C, whereas the tenth percentile of temperatures in habitats occupied by arrowtooth flounder typically exceeds 2°C. In contrast, juvenile pollock do not show strong avoidance of low temperatures, although do seem to show a slightly more limited range of temperature than the available temperatures (i.e. the tenth percentile and 90th percentile points fall slightly above and below the 1:1 line, respectively).

Avoidance of the cold pool by arrowtooth flounder results in a larger percentage (by number) of the stock in the SE outer shelf as the cold pool area increases, and a reduced percentage in the SE middle shelf (Figure 3). For arrowtooth flounder <40 cm, the

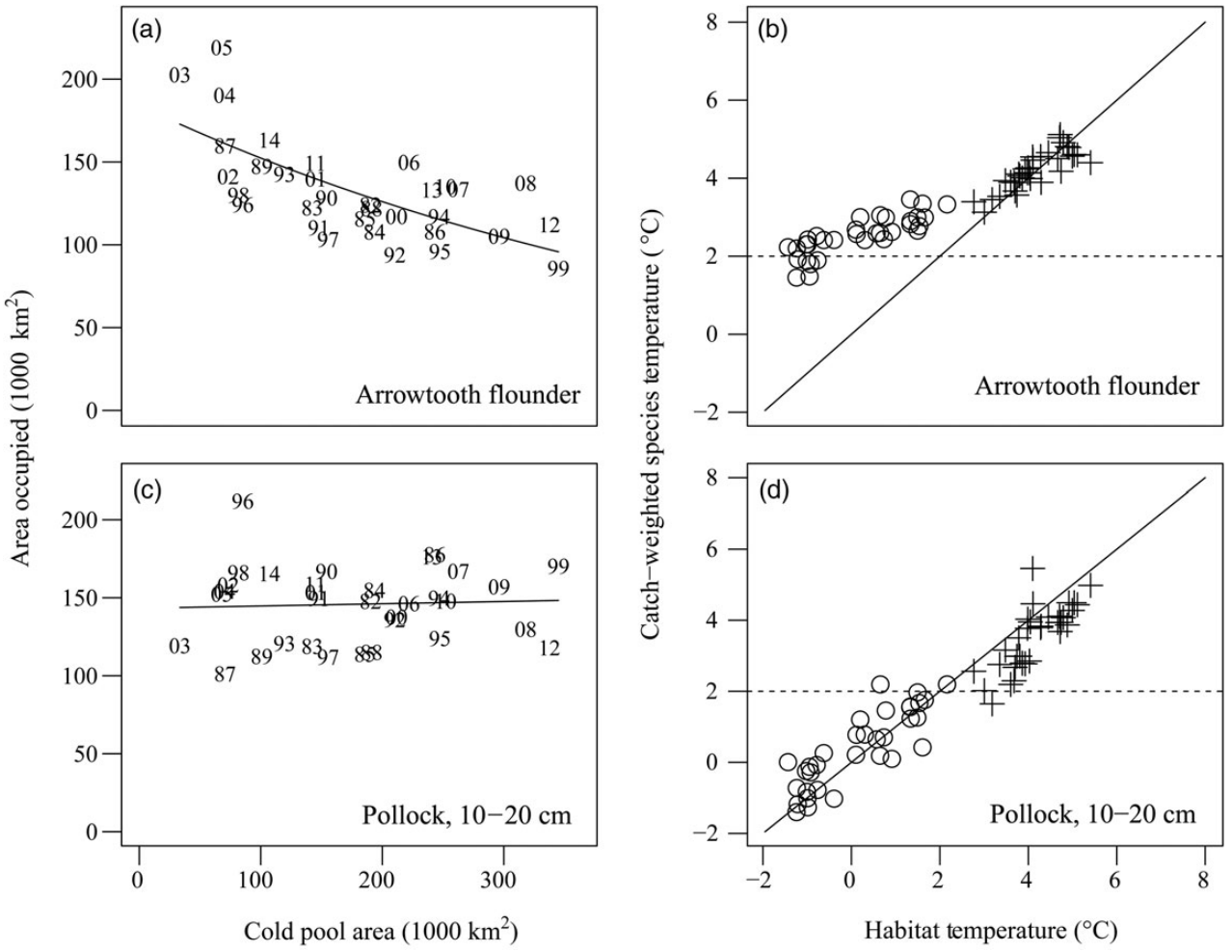

Figure 2. The relationship between the area occupied and cold pool area for arrowtooth flounder and juvenile walleye pollock (a and c, labelled by year). Scatterplots of the bottom temperatures for the tenth (○) and 90th (+) percentiles of the distributions of available temperatures and the catch-weighted temperature distributions are in (b) and (d). Temperature preference in indicated by deviations from the 1:1 line, and points below the horizontal lines indicate species occurrence within the cold pool.

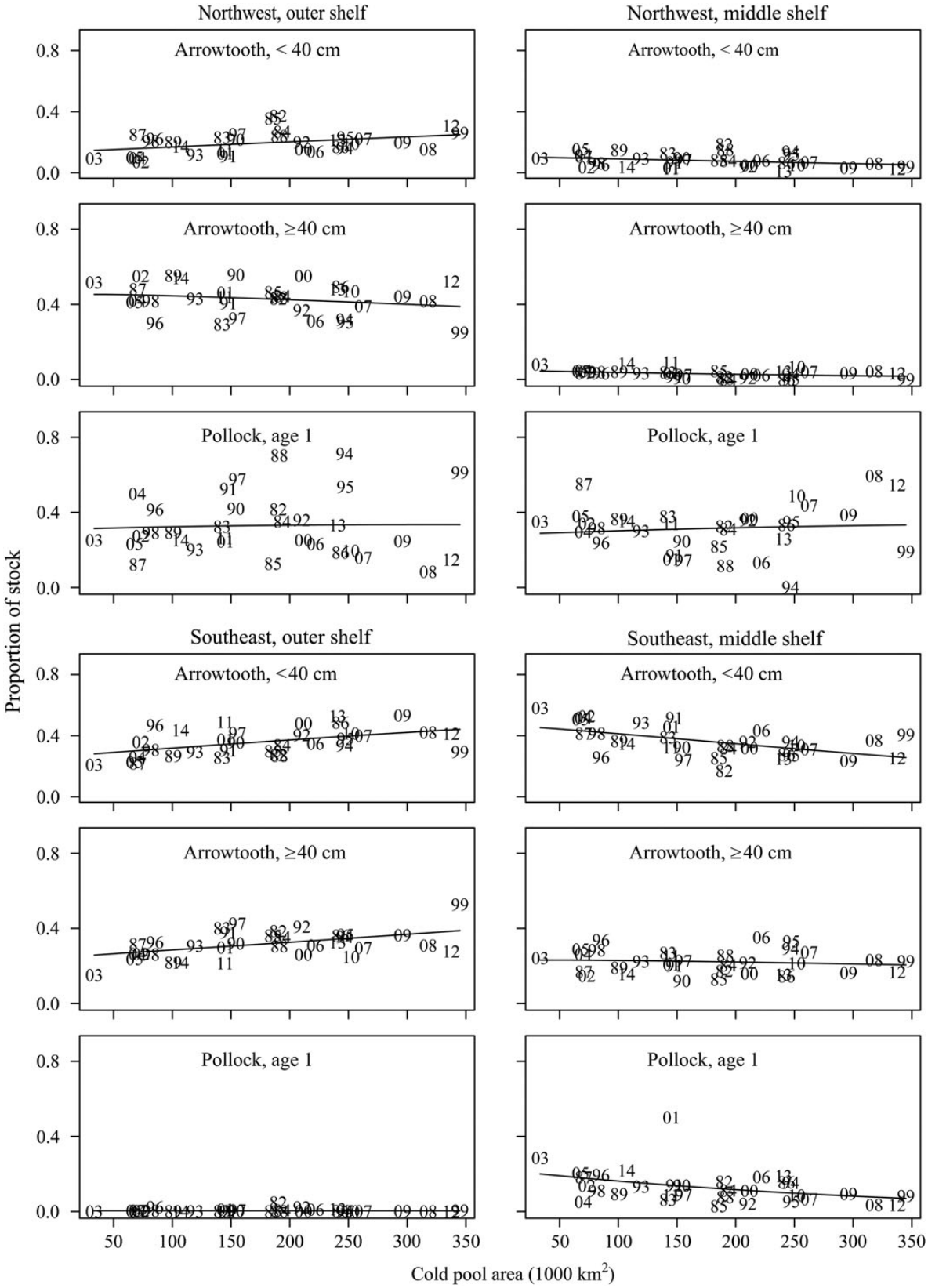

Figure 3. The proportion (by number) of two size classes of arrowtooth flounder, and age 1 pollock, across areas within the EBS shelf (labelled by year), with fitted lines obtained from a multinomial logistic model.

modelled percentage in the SE middle shelf declines from 45 to 26%, whereas the percentage in the SE outer shelf increases from 28 to 44%, and the percentage in the NW outer shelf increases from 15 to 25%. Large arrowtooth flounder (≥40 cm) show an increase (26 to 39%) in the SE outer shelf with increasing cold pool area and slight declines in other areas. In contrast, the distribution of age-1 walleye pollock is less sensitive to changes in the cold pool. The areas of highest densities of age-1 pollock are the NW outer shelf and NW middle shelf, where the modelled percentage of the stock varies from 31–34% and 29–33%, respectively. Age-1 pollock are less abundant in the SE middle and SE outer shelf, and the percentage of age-1 pollock in the SE middle shelf declines from 20 to 7% as the area of the cold pool increases.

The consumption equation (equation 5) can be rearranged to express modelled consumption per predator and area as a function of prey density (i.e. the type II predator functional response), which exhibited a variety of shapes across the combinations of arrowtooth size and pollock age (Figure 4) that reflects its flexibility to fit the input data on estimated predator consumption. Small arrowtooth flounder had a saturating functional response for consumption of age-1 pollock, a linear functional response for age-2 pollock, and a relatively constant but low functional response on age-3 pollock at prey densities >30,000 km^{-2}. The estimated consumption rates of large arrowtooth flounder exceeded those of small arrowtooth flounder. The highest rates of consumption were estimated for large arrowtooth flounder on age-1 pollock, with a modelled annual rate exceeding 0.25 pollock consumed per 1000 arrowtooth flounder per km^2 at high pollock densities. The lowest consumption rates were estimated for small arrowtooth flounder on age-3 pollock with a modelled asymptotic rate <0.002 pollock consumed per 1000 arrowtooth flounder per km^2.

The estimated recruitment of age-1 pollock was reduced at either high or low temperatures, and the estimated parameters for the quadratic relationship in equation (3) were $\theta_0 = -32.7$, $\theta_1 = 7.4$, and $\theta_2 = -0.42$ (Figure 5). The predicted value of recruitment at the largest SST observed since 1962 (10.4°C, observed in 2005) is 34% of the predicted recruitment at the peak of the quadratic relationship, which occurs at 8.8°C. The decline in predicted recruitment at low temperatures is a result of several years in the early 1970s (1970–1973 and 1975–1976) which had both low temperatures and low recruitment residuals.

Model estimates of time-series of estimated natural mortality for pollock ages 1–3 show an increase over time (Figure 6), which reflects the threefold increase of arrowtooth flounder from 1977 to 2014 (Spies *et al.*, 2014). The estimated mortality rates of age-1 pollock for the 1980–1989 and 2000–2013 periods were 0.92 and 1.07 yr^{-1}, respectively, representing a 16% increase in the recent period; for ages 2 and 3, the per cent increases between these periods were estimated at 29 and 36%, respectively. The largest values of age-1 predation mortality occurred during warm years of 2003–2005, which can be attributed to several factors including a relatively large proportion of small arrowtooth and age 1 pollock

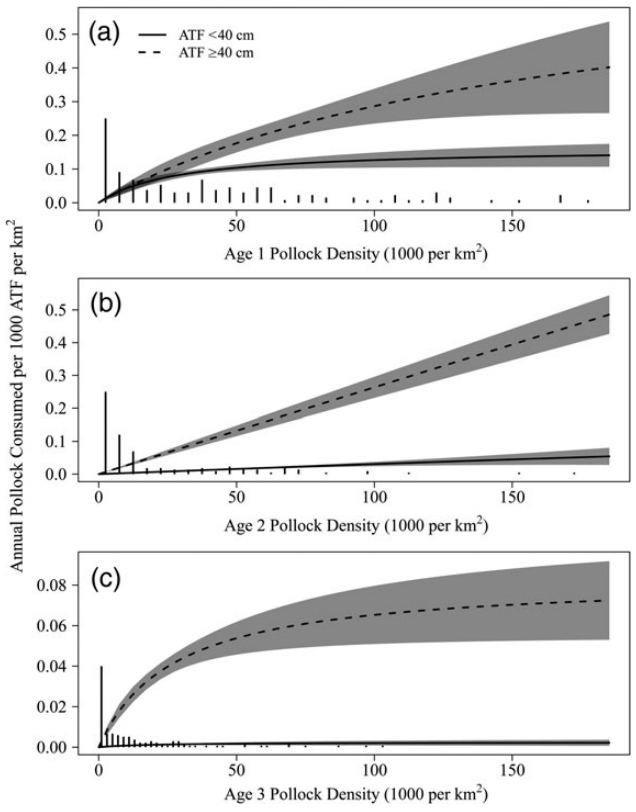

Figure 4. Estimated functional response curves and 95% confidence intervals for predation by two arrowtooth flounder size classes on three pollock age groups; temperature and fish weights were set to their average value from 1982 to 2014. Vertical bars are histograms of model-estimated subarea pollock density from 1983 to 2012 plotted on a relative scale.

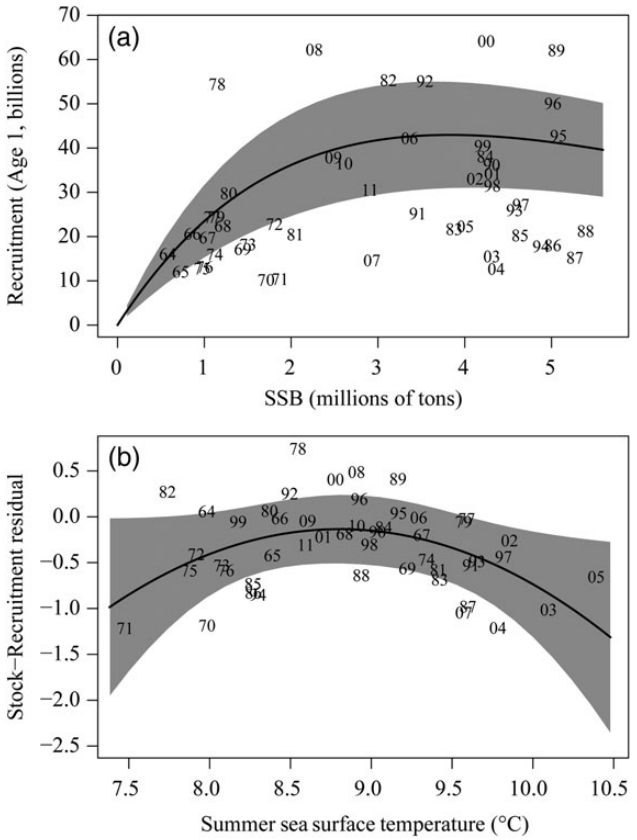

Figure 5. The estimated Ricker stock–recruitment curve for walleye pollock (a), accounting for the effect of SST on the recruitment residuals (b). Data points are labelled by year class, and the shaded areas are 95% confidence intervals.

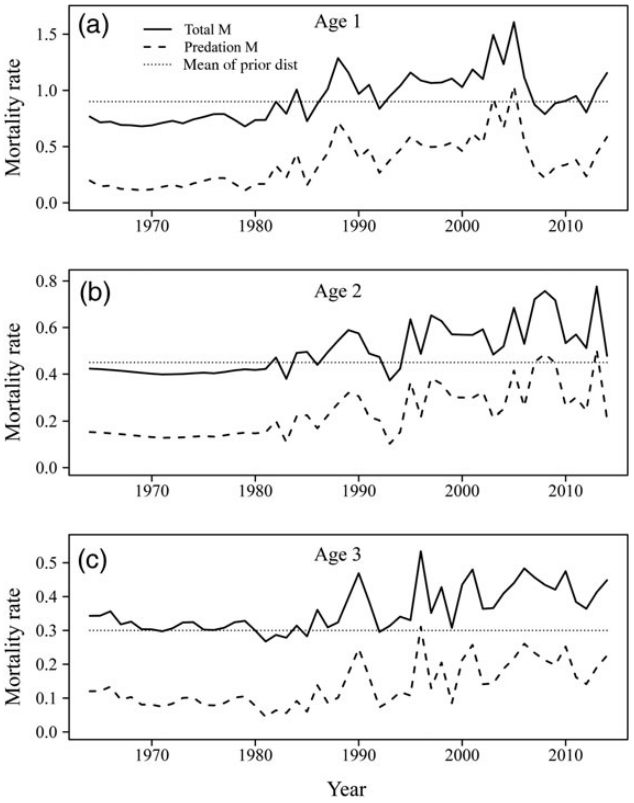

Figure 6. Estimated arrowtooth flounder predation mortality (dashed line) and total mortality (solid line) by year for pollock ages 1–3; the mean of the prior distribution for total mortality is shown with the dotted line.

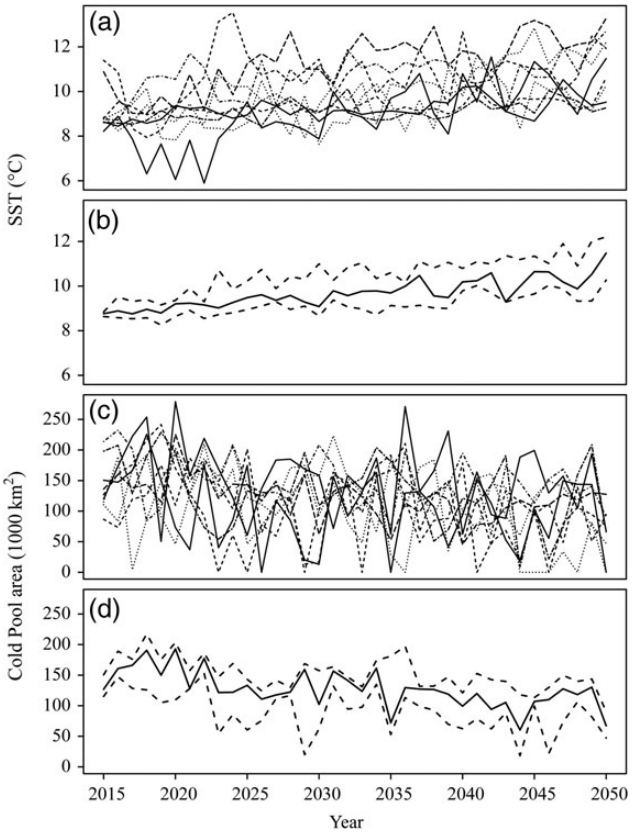

Figure 7. Projections of EBS SST (a) and cold pool area (c) obtained from nine GCMs, with the median and interquartile distance by year shown in (b) and (d).

in the SE middle shelf in 2003 (Figure 3), the increased levels of the maximum rate of consumption in 2003–2005 due to high temperatures, and the lower abundance of age-1 pollock in 2004 and 2005; the latter two factors increase the predator catchability and hence morality rates of pollock by arrowtooth flounder.

The projected environmental conditions from 2015 to 2050 show warming, with SST increasing and cold pool area decreasing (Figure 7). The median of projected SST from the nine climate models from 2045 to 2050 was 1.8°C larger than the median from 2015 to 2020. Similarly, the median of projected cold pool area from 2045 to 2050 was 31% smaller than the median from 2015 to 2020. The cold pool area during the unusually warm years of 2003–2005 (average of 58,900 km^2) would fall within the interquartile distance for 3 of the 7 projected years from 2044 to 2050.

When the maximum rate of consumption, predator–prey spatial overlap, and pollock recruitment are projected as function of environmental conditions (referred to as the base projection below), the projected pollock biomass and catch decrease (Figure 8). The mean projected biomass in 2050 is 5800 kt, decreasing from the initial projection biomass of 17,000 kt in 2014. The projected predation mortality on age-1 pollock increases, which can be attributed to the increase in predator catchability associated with smaller pollock stock sizes. The CV of projected biomass increases through the projection period due to the decline in mean projected biomass, and is ~0.6 in 2050 (Figure 8).

The effect of SST on recruitment has a stronger influence on pollock dynamics than the effect of bottom temperatures and cold pool area on either the maximum consumption rate or predator–prey spatial overlap. When only recruitment is projected as environmentally dependent, the projected biomass for 2050 is <10% larger relative to the base projection (Figure 8). However, the projected predation mortality is more substantially reduced (a 23% reduction in the mean of projected values for 2050) because of the absence of an environmental effect on predator and prey spatial distributions. Projections that only modify the predator–prey spatial distributions based on the cold pool area, or the maximum rate of consumption based on bottom temperatures, have much larger pollock biomass and catch due to the absence of an environmental effect on pollock recruitment. The CV of mean biomass for these projections is ~0.2 for years beyond 2020.

The proportion of arrowtooth flounder which occur in the NW middle shelf typically does not exceed 10% even in the warmest years observed, although this is an area with a substantial portion of the age-1 pollock (average of 31% from 1982 to 2014; Figure 3). The sensitivity analysis producing a greater rate of northward movement resulted in the predicted proportion of small and large arrowtooth flounder in the NW middle shelf during the year with the smallest observed cold pool (2003) of 24 and 22%, respectively, an increase from the estimated values of 10 and 5% (Figure 9). The rate of northward movement for this sensitivity analysis projection (not shown) was <0.01° latitude per year (assuming the trend in the median cold pool area from the ensemble in Figure 7). This change in modelled response of arrowtooth flounder spatial distribution to the cold pool decreased the projected mean pollock biomass and catch in 2050 by 10 and 17%, respectively, relative to the base projection (Figure 8). The mean of projected age-1 predation mortality rates

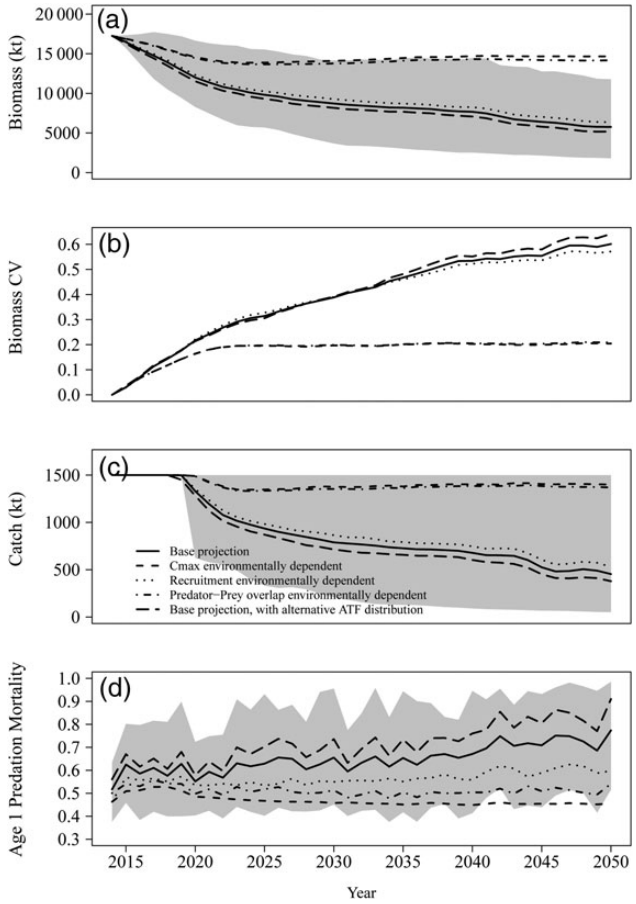

Figure 8. Projections of mean biomass (a), CV of biomass (b), mean catch (c), and mean age-1 predation mortality (d) from 2014 to 2050 for EBS walleye pollock. The base projection, and base projection with the alternative arrowtooth flounder distribution, includes environmental effects on maximum consumption rate, recruitment, and predator–prey spatial overlap. Other projections model environmental effects only on a single mechanism. The shaded areas are the distance between the fifth and 95th percentiles from the simulations with the base model.

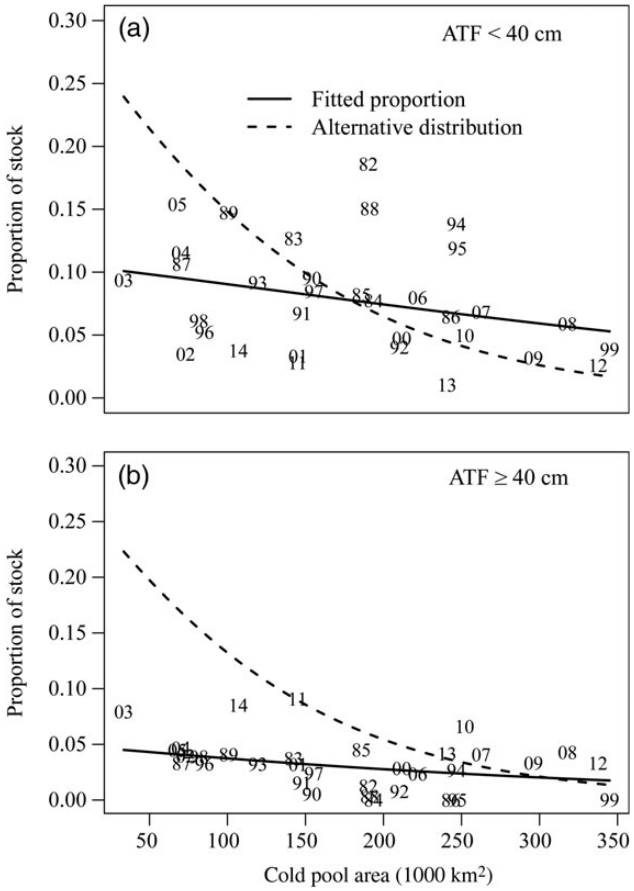

Figure 9. The observed (labelled by year) and modelled proportion of small (a) and large (b) arrowtooth flounder in the NW middle shelf; the dashed lines are alternative distributions of arrowtooth flounder that are used in a sensitivity run for pollock projections.

under this sensitivity analysis increased by 18% relative to the base projection due to a greater predator–prey overlap under future warm years.

Discussion

Environmentally enhanced single-species statistical population assessment models can serve as useful tools for teasing apart the myriad ways that environmental variability can affect the population dynamics of marine fish. In this example application, trends in temperature were evaluated with respect to their effect on recruitment of pollock (i.e. survival to age 1), the maximum rate of consumption of arrowtooth flounder, and the overlap between arrowtooth flounder and juvenile pollock. Of the processes considered, the effect of temperature on pollock recruitment had the largest impact on projected future dynamics, consistent with recruitment modelling conducted by Mueter *et al.* (2011) that indicated that projected future recruitment, spawning biomass, and catch declined when the effect of SST on pollock recruitment was considered. Mueter *et al.* (2011) also found that projected future recruitment declines with increased arrowtooth flounder abundance via a spatially aggregated predation index that was used a covariate in the Ricker stock–recruitment model. In this study, the availability of data on diet and stock distributions allowed estimation of predator functional response curves and predation mortality rates by subarea and prey age, which arise from the overlap of predator and prey spatial distributions. Many fish stocks would be expected to have spatial distributions affected by trends in environmental conditions (Dulvy *et al.*, 2008; Mueter and Litzow, 2008; Nye *et al.*, 2009). In these cases, the methodology demonstrated in this study is an approach for assessing the effect of environmental trends on predator–prey overlap and predation mortality, and distinguishing the effects of environmental trends on post-recruitment mortality from the effects on prerecruitment mortality.

Of the processes considered here that relate environmental variables to pollock dynamics, the dominance of the SST–recruitment relationship on projected future abundance is not unexpected given the different ages at which these processes occur. The effect of SST on recruitment occurs at a younger age when cohort abundance and natural mortality rates are relatively large and where a given percentage change in mortality will be highly influential in determining relative year-class strength. These results emphasize that the overall scale of year-class abundance is largely determined by prerecruit density-independent mortality, with prerecruit density-dependent mortality further adjusting recruitment strength (Houde, 2008, 2009). Although temperature can have direct effects on prerecruit

mortality via physiology, behaviour, growth, and stage duration (Houde, 1989; Pepin, 1991), high SST in the EBS shelf is largely thought of as an indirect effect reflecting reduced abundances of *Calanus* copepods and other zooplankton in the late summer period that affects the overwinter survival to age 1 (Hunt *et al.*, 2011; Mueter *et al.*, 2011; Heintz *et al.*, 2013). Despite the importance of environmentally driven recruitment trends on total abundance, the role of environmentally driven patterns in predation mortality can potentially alter post-recruit abundance, particularly in cases where substantial changes occur in species distributions and predator–prey overlap as a result of climate change.

The stock projections produced here are affected by many sources of variability, including uncertainty in future projections of SST, cold pool area, and bottom temperatures, and the process error residuals associated with the environmentally driven predictions of recruitment. We followed the established practice of using an ensemble of climate models to represent uncertainty in future climate projections (e.g. Parker, 2013). Further refinements could incorporate uncertainty in the estimation of stock–recruitment parameters, the Holling type II functional response parameters, and the multinomial logistic parameters relating predator and prey spatial distributions to the cold pool area. Because these uncertainties were not considered in the projections to focus on effects due to climate change, the variability in the projected quantities is underestimated. Ianelli *et al.* (2011) also incorporated uncertainty in future environmental conditions into stock projection models and found some alternative harvest strategies that outperformed the current harvest control rule when EBS walleye pollock recruitment is affected by temperature.

The potential for predation on walleye pollock to be affected by climate change depends both on the degree to which environmental conditions will change in the EBS shelf and its effect on the spatial distributions of walleye pollock and their predators. Analyses of physical and biological data indicate areas south of ~60°N (which include most of the EBS shelf survey data considered here) will be most strongly affected by climate change through loss of less sea ice, and thus a reduction in the cold pool in the middle shelf, although large interannual variability is expected (Stabeno *et al.*, 2012). These results are consistent with the downscaled climate projections shown in Figure 7, which indicate that years such as 2003–2005, which were perceived as unusually warm when they occurred, are expected to occur with higher frequency in the future.

Movement to new locations would be expected to vary among individuals within a stock, resulting in the case seen here where the area occupied by arrowtooth flounder varied with temperature (Figure 2). This could occur if individuals closest to their thermal tolerances, and/or geographically close to areas with lower abundances and thus less competition (i.e. density-dependent habitat selection; MacCall, 1990), were more likely to move to new habitats. Although the variability in the directional movement of marine species has often been attributed to biological characteristics (Murawski, 1993; Perry *et al.*, 2005), density-dependent habitat selection is a potential factor influencing changes in spatial distributions (Spencer, 2008), particularly in cases where land boundaries and/or thermal constraints (i.e. the cold water on the northern EBS shelf; Stabeno *et al.*, 2012) would force movement in a particular direction. The effects of density-independent and density-dependent factors can also interact; for example, Ciannelli *et al.* (2012) observed that in recent years the effect of biomass on the spatial distribution of EBS arrowtooth flounder depends on temperature. The model presented here can provide information on how changes in densities across various subareas could affect predation and population dynamics.

It is unclear the extent to which currently observed relationships between arrowtooth flounder spatial distributions and cold pool area would apply to different environmental conditions in the future. The sensitivity analysis in which the proportion of arrowtooth flounder in the NW middle shelf is increased during warm years would result in a rate of northward movement ($<0.01^\circ$ latitude per year) that is generally consistent with rates of latitudinal shifts from other marine ecosystems off North America (Pinsky *et al.*, 2013). However, because this movement is into an area that contains a relatively large portion of the juvenile pollock population, the predation mortality would be increased to a greater extent than would occur under the current relationship between the spatial distribution of arrowtooth flounder and the cold pool. Movement of pollock and arrowtooth flounder to areas north of ~60°N is not expected because this area is likely to remain cold with extensive ice cover in the foreseeable future (Stabeno *et al.*, 2012). However, the broad extent and spatial variability of temperature on the EBS shelf indicate that fish stocks on the southern EBS shelf (i.e. south if 60° N; Stabeno *et al.*, 2012) may be able to find suitable temperatures without necessarily moving along a single axis (Kotwicki and Lauth, 2013). This might explain community-level analyses indicating wide variation in the directional movement among species in the EBS (Pinsky *et al.*, 2013), with many species showing no significant latitudinal trend in their distribution (Mueter and Litzow, 2008).

The method used in this study to estimate spatially explicit predation mortality rates is applicable to data-rich stocks, as it requires field data on stomach contents (in addition to the data necessary for age-structured stock assessments). In addition to producing the C_{max} estimates used in this study that were based on a generalized von Bertalanffy growth function (Pauly, 1981; Essington *et al.*, 2001), Holsman and Aydin (2015) also estimated C_{max} from: (i) field-based approaches that relied on digestion equations and evacuation rates (Elliot and Persson, 1978; Durbin *et al.*, 1983); (ii) a bioenergetics model (Hanson *et al.*, 1997); and (iii) a specialized von Bertalanffy growth function (Ursin, 1967; Pauly, 1981). Some variability exists in the resulting estimates; for example, Holsman and Aydin (2015) found that C_{max} for arrowtooth flounder $\geq$40 cm differed by a factor of 4 between the five methods they evaluated. An advantage of estimating spatially explicit predation mortality within the assessment model is that uncertainties in the diet data, and estimated predator abundance, can be quantified relative to other input data, and adds an additional data component to be evaluated when determining data weights (Francis, 2011). A simpler alternative to using survey data to infer the time-varying predator–prey overlap (via the type II functional response) is to assume that the overlap is constant or a simple function of temperature. Although arrowtooth flounder clearly avoid the cold pool, the distribution of juvenile pollock is less sensitive to temperature (a result also observed from GAM models; Hunsicker *et al.*, 2013), resulting in a variable relationship between simple measures of overlap and temperature.

Because arrowtooth flounder are the only predator of pollock considered in this study, it is not clear that the total natural mortality rates of juvenile pollock have been increasing over time. Multispecies models that include Pacific cod and cannibalism of pollock on ages 1 and older indicate that the predation mortality from these two sources have been decreasing over time, with the overall natural mortality rate variable but without a noticeable trend (Holsman *et al.*, in press). A significant portion of the

cannibalism is modelled within the Ricker stock–recruitment function, and additional predators could easily be added to the model to further partition the residual natural mortality. The approach taken here of using current estimates of total natural mortality at age to constrain the estimates of residual and predation mortality was motivated by empirical relationships between total natural mortality and length at age (Lorenzen, 2000), and a logistic model for natural mortality of older fish that is scaled to maturation (Lehodey *et al.*, 2008). These estimates are qualitatively similar but are lower at younger ages and higher at older ages than those obtained from the method of Gislason *et al.* (2010) relating total natural mortality to growth parameters and size at age.

The model presented here is intermediate in complexity between traditional single-species models in which data on diet and predator–prey overlap are typically omitted when obtaining estimates of natural mortality, and multispecies models that characterize the dynamics of several interacting species. Models of intermediate complexity for ecosystem (MICE) assessments have been developed in other regions (Plaganyi *et al.*, 2011). Relative to more complex multispecies models, the MICE models may ease the task of incorporating species interactions (and their potential relationship with environmental variables) into stock assessment and management. Further work should be conducted to evaluate management strategies for stocks which have identified environmental drivers of key biological processes (Ianelli *et al.*, 2011), potentially including the effects of the environment on predator–prey spatial overlap. A primary focus of the model in this study is to obtain improved estimates of natural mortality and abundance for a given species, whereas multispecies models with full feedback between interacting predator and prey species are ideally suited to characterizing system dynamics and evaluating trade-offs in multispecies harvesting strategies (Link and Browman, 2014). The model presented in this study could be improved by more fully evaluating the data weighting and variability of the consumption input data relative to other data inputs.

Supplementary data

Supplementary material is available at the *ICESJMS* online version of the manuscript.

Acknowledgements

We thank Carey McGilliard, Ingrid Spies, and Martin Dorn for helpful discussions and comments on previous drafts of this paper.

References

Baker, M. R., and Hollowed, A. B. 2014. Delineating ecological regions in marine systems: Integrating physical structure and community composition to inform spatial management in the eastern Bering Sea. Deep-Sea Research II, 109: 215–240.

Brander, K. M. 2007. Global fish production and climate change. Proceedings of the National Academy of Sciences of the United States of America, 104: 19709–19714.

Ciannelli, L., Bartolino, V., and Chan, K.-S. 2012. Non-additive and non-stationary properties in the spatial distribution of a large marine fish population. Proceedings of the Royal Society of London B. 279: 3635–3642.

Dulvy, N. K., Rogers, S. I., Jennings, S., Stelzenmuller, V., Dye, S. R., and Skjoldal, H. R. 2008. Climate change and deepening of the North Sea assemblage: a biotic indicator of warming seas. Journal of Applied Ecology, 45: 1029–1039.

Durbin, E. G., Durbin, A. G., Langton, R. W., and Bowman, R. E. 1983. Stomach contents of silver hake, *Merluccius bilinearis*, and Atlantic cod, *Gadus morhua*, and estimation of their daily rations. Fishery Bulletin, 81: 437–454.

Elliot, J., and Persson, L. 1978. The estimation of daily rates of food consumption for fish. Journal of Animal Ecology, 47: 977–991.

Essington, T. E., Kitchell, J. F., and Walters, C. J. 2001. The von Bertalanffy growth function, bioenergetics, and the consumption rates of fish. Canadian Journal of Fisheries and Aquatic Sciences, 58: 2129–2138.

Francis, R. I. C. C. 2011. Data weighting in statistical fisheries stock assessment models. Canadian Journal of Fisheries and Aquatic Sciences, 68: 1124–1138.

Gislason, H., Daan, N., Rice, J. C., and Pope, J. G. 2010. Size, growth, temperature and the natural mortality of marine fish. Fish and Fisheries, 11: 149–158.

Hanson, P., Johnson, T., Schindler, D., and Kitchell, J. 1997. Fish Bioenergetics v.3.0. University of Wisconsin Sea Grant Institute, Madison, WI.

Heintz, R. A., Siddon, E. C., Farley, R. V., Jr., and Napp, J. M. 2013. Correlation between recruitment and fall condition of age-0 pollock (*Theragra chalcogramma*) from the eastern Bering Sea under varying climate conditions. Deep-Sea Research II, 94: 150–156.

Hoegh-Guldberg, O., Cai, R., Poloczanska, E. S., Brewer, P. G., Sundby, S., Hilmi, K., Fabry, V. J., *et al.* 2014. The ocean. *In* Climate Change 2014: Impacts, Adaptation, and Vulnerability. Part B: Regional Aspects. Contribution of Working Group II to the Fifth Assessment Report of the Intergovernmental Panel on Climate Change, pp. 1655–1731. Ed. by V. R. Barros, C. B. Field, D. J. Dokken, M. D. Mastrandrea, K. J. Mach, T. E. Bilir, M. Chatterjee, *et al.* Cambridge University Press, Cambridge, UK and New York, NY, USA.

Hollowed, A. B., Barbeaux, S. J., Cokelet, E. D., Farley, E., Kotwicki, S., Ressler, P. H., Spital, C., and Wilson, C.D. 2012. Effects of climate variations on pelagic ocean habitats and their role in structuring forage fish distributions in the Bering Sea. Deep-Sea Research II, 65–70: 230–250.

Hollowed, A. B., Ianelli, J. N., and Livingston, P. A. 2000. Including predation mortality in stock assessments: a case study for Gulf of Alaska walleye pollock. ICES Journal of Marine Science, 57: 279–293.

Holsman, K. K., and Aydin, K. 2015. Comparative methods for evaluating climate change impacts on the foraging ecology of Alaskan groundfish. Marine Ecology Progress Series, 521: 217–235.

Holsman, K. K., Ianelli, J., Aydin, K., Punt, A. E., and Moffit, E. A. in press. A comparison of fisheries biological reference points estimated from temperature-specific multi-species and single-species climate-enhanced stock assessment models. Deep-Sea Research II, doi:10.1016/j.dsr2.2015.08.001.

Hosmer, D. W., and Lemeshow, S. 2000. Applied Logistic Regression, 2nd Ed. Wiley, New York. 373 pp.

Houde, E. D. 1989. Comparative growth, mortality, and energetic of marine fish larvae: temperature and implied latitudinal effects. Fishery Bulletin, 87: 471–495.

Houde, E. D. 2008. Emerging from Hjort's shadow. Journal of the Northwest Atlantic Fisheries Science, 41: 53–70.

Houde, E. D. 2009. Recruitment variability. *In* Fish Reproductive Biology and Its Implications for Assessment and Management, pp. 91–171. Ed. by T. Jakobsen, M. Fogarty, B. A. Megrey, and E. MoksnessWiley-Blackwell, Oxford. 440 pp.

Hunsicker, M. E., Ciannelli, L., Bailey, K. M., Zador, S., and Stige, L. C. 2013. Climate and demography dictate the strength of predator-prey overlap in a subarctic marine ecosystem. PLoS ONE, 8: e66025.

Hunt, G. L., Coyle, K. O., Eisner, L. B., Farley, E. V., Heintz, R. A., Mueter, F., Napp, J. M., *et al.* 2011. Climate impacts on eastern Bering Sea foodwebs: a synthesis of new data and an assessment of the Oscillating Control Hypothesis. ICES Journal of Marine Science, 68: 1230–1243.

Hunt, G. L., Stabeno, P., Walters, G., Sinclair, E., Brodeur, R. D., Napp, J. M., and Bond, N. A. 2002. Climate change and control of the southeastern Bering Sea pelagic ecosystem. Deep-Sea Research II, 49: 5821–5853.

Hunt, G. L., Stabeno, P. J., Strom, S., and Napp, J. M. 2008. Patterns of spatial and temporal variation in the marine ecosystem of the

southeastern Bering Sea, with special reference to the Pribilof Domain. Deep-Sea Research II, 55: 1919–1944.

Ianelli, J. N., Barbeaux, S., Honkalehto, T., Kotwicki, S., Aydin, K., and Williamson, N. 2009. Assessment of the walleye stock in the eastern Bering Sea. *In* Stock Assessment and Fishery Evaluation Report for the Groundfish Resources of the Bering Sea/Aleutian Islands Regions, pp. 49–147. North Pacific Fishery Management Council, Anchorage, AK.

Ianelli, J. N., Hollowed, A. B., Haynie, A. C., Mueter, F. J., and Bond, N. A. 2011. Evaluating management strategies for eastern Bering Sea walleye pollock (*Theragra chalcogramma*) in a changing environment. ICES Journal of Marine Science, 68: 1297–1304.

Ianelli, J. N., Honkalehto, T., Barbeaux, S., and Kotwicki, S. 2014. Assessment of the walleye stock in the eastern Bering Sea. *In* Stock Assessment and Fishery Evaluation Report for the Groundfish Resources of the Bering Sea/Aleutian Islands Regions, pp. 55–156. North Pacific Fishery Management Council, Anchorage.

Kotwicki, S., and Lauth, R. L. 2013. Detecting temporal trends and environmentally-driven changes in the spatial distribution of bottom fishes and crabs on the eastern Bering Sea shelf. Deep-Sea Research II, 94: 231–243.

Lauth, R. R., and Conner, J. 2014. Results of the 2011 Eastern Bering Sea continental shelf bottom trawl survey of groundfish and invertebrate fauna. U.S. Department of Commerce NOAA Technical Memorandum NMFSAFSC-266. 176 pp.

Lehodey, P., Senina, I., and Murtugudde, R. 2008. A spatial ecosystem and populations dynamics model (SEAPODYM)—Modeling of tuna and tuna-like populations. Progress in Oceanography, 78: 304–318.

Link, J. S., and Browman, H. I. 2014. Integrating what? Levels of marine ecosystem-based assessment and management. ICES Journal of Marine Science, 71: 1170–1173.

Loarie, S. R., Duffy, P. B., Hamilton, H., Asner, G. P., Field, C. B., and Ackerly, D. D. 2009. The velocity of climate change. Nature, 462: 1052–1055.

Lomas, M. W., and Stabeno, P. J. 2014. An introduction to the Bering Sea project: volume III. Deep-Sea Research II, 109: 1–4.

Lorenzen, K. 2000. Allometry of natural mortality as a basis for assessing optimal release size in fish stocking programmes. Canadian Journal of Fisheries and Aquatic Sciences, 57: 2374–2381.

MacCall, A. D. 1990. Dynamic Geography of Marine Fish Populations. University of Washington Press, Seattle, WA. 153 pp.

Maunder, M. N., and Punt, A. E. 2013. A review of integrated analysis in fisheries stock assessment. Fisheries Research, 142: 61–74.

Mueter, F. J., Bond, N. A., Ianelli, J. N., and Hollowed, A. B. 2011. Expected declines in recruitment of walleye pollock (*Theragra chalcogramma*) in the eastern Bering Sea under future climate change. ICES Journal of Marine Science, 68: 1284–1296.

Mueter, F. J., and Litzow, M. A. 2008. Warming climate alters the biogeography of the Bering Sea continental shelf. Ecological Applications, 18: 309–320.

Murawski, S. A. 1993. Climate change and marine fish distributions: forecasting from historical analogy. Transactions of the American Fisheries Society, 122: 647–658.

NPFMC (North Pacific Fishery Management Council). 2014. Stock assessment and fishery evaluation report for the groundfish resources of the Bering Sea/Aleutian Islands regions. North Pacific Fishery Management Council, Anchorage, AK. 2000 pp.

Nye, J. A., Link, J. S., Hare, J. A., and Overholtz, W. J. 2009. Changing spatial distribution of fish stocks in relation to climate and population size on the Northeast United States continental shelf. Marine Ecology Progress Series, 393: 111–129.

Overland, J. E., and Wang, M. 2007. Future regional Arctic Sea ice declines. Geophysical Research Letters, 34: L17705.

Parker, W. S. 2013. Ensemble modeling, uncertainty and robust predictions. Wiley Interdisciplinary Reviews: Climate Change, 4: 213–223.

Pauly, D. 1981. The relationship between gill surface area and growth performance in fish: a generalization of von Bertalanffy's theory of growth. Meeresforschung, 28: 251–282.

Pepin, P. 1991. Effect of temperature and size on development, mortality, and survival rates of the pelagic early life history stages of marine fish. Canadian Journal of Fisheries and Aquatic Sciences, 48: 503–518.

Perry, A. L., Low, P. J., Ellis, J. R., and Reynolds, J. D. 2005. Climate change and distribution shifts in marine fishes. Science, 308: 1912–1915.

Perry, R. I., and Smith, S. J. 1994. Identifying habitat associations of marine fishes using survey data: an application to the northwest Atlantic. Canadian Journal of Fisheries and Aquatic Sciences, 51: 589–602.

Pinsky, M. L., Worm, B., Fogarty, M. J., Sarmiento, J. L., and Levin, S. A. 2013. Marine taxa track local climate velocities. Science, 341: 1239–1242.

Plaganyi, E. E., Bell, J. D., Bustamante, R. H., Dambacher, J. M., Dennis, D. M., Dichmont, C. M., Dutra, L. X. C., *et al.* 2011. Modelling climate-change effects on Australian and Pacific aquatic ecosystems: a review of analytical tools and management implications. Marine and Freshwater Research, 62: 1132–1147.

Ricker, W. E. 1975. Computation and interpretation of biological statistics of fish populations. Bulletin of the Fisheries Research Board of Canada 191. 382 pp.

Rose, K. A., Megrey, B. A., Hay, D., Werner, F., and Schweigert, J. 2008. Climate regime effects on Pacific herring growth using coupled nutrient–phytoplankton–zooplankton and bio-energetics models. Transactions of the American Fisheries Society, 137: 278–297.

Smith, T. M., Reynolds, R. W., Peterson, T. C., and Larimore, J. 2008. Improvements to NOAA's historical merged land-ocean surface temperature analysis (1880–2006). Journal of Climate, 21: 2283–2296.

Spencer, P. D. 2008. Density-independent and density-dependent factors affecting temporal changes in spatial distributions of eastern Bering Sea flatfish. Fisheries Oceanography, 17: 396–410.

Spies, I., Wilderbuer, T. K., Nichol, D. G., and Aydin, K. 2014. Arrowtooth flounder. *In* Stock Assessment and Fishery Evaluation Report for the Groundfish Resources of the Bering Sea/Aleutian Islands Regions, pp. 921–1012. North Pacific Fishery Management Council, Anchorage, AK.

Stabeno, P. J., Bond, N. A., Kachel, N. B., and Salo, S. A. 2001. On the temporal variability of the physical environment over the southeastern Bering Sea. Fish. Oceanogr. 10: 81–98.

Stabeno, P. J., Farley, E. V., Kachel, N. B., Moore, S., Mordy, C. W., Napp, J. M., Overland, J. E., *et al.* 2012. A comparison of the physics of the northern and southern shelves of the eastern Bering Sea and some implications for the ecosystem. Deep-Sea Research II, 65–70: 14–30.

Stocker, T. F., Qin, D., Plattner, G-K., Alexander, L. V., Allen, S. K., Bindoff, N. L., Bréon, F-M., *et al.* 2013. Technical Summary. *In* Climate Change 2013: The Physical Science Basis. Contribution of Working Group I to the Fifth Assessment Report of the Intergovernmental Panel on Climate Change, pp. 33–115. Ed. by T. F. Stocker, D. Qin, G.-K. Plattner, M. Tignor, S. K. Allen, J. Boschung, A. Nauels, *et al.* Cambridge University Press, Cambridge, UK and New York, NY, USA.

Swain, D. P., and Sinclair, A. F. 1994. Fish distribution and catchability: what is the appropriate measure of distribution? Canadian Journal of Fisheries and Aquatic Sciences, 51: 1046–1054.

Ursin, E. 1967. A mathematical model of some aspects of fish growth, respiration, and mortality. Journal of the Fisheries Research Board of Canada, 24: 2355–2453.

Wyllie-Echeverria, T., and Wooster, W. S. 1998. Year-to-year variations in Bering Sea ice cover and some consequences for fish distributions. Fisheries Oceanography, 7: 159–170.

Zador, S., Aydin, K., and Cope, J. 2011. Fine-scale analysis of arrowtooth flounder (*Atherestes stomias*) catch-pet-unit-effort reveals spatial trends in abundance. Marine Ecology Progress Series, 438: 229–239.

Handling editor: Valerio Bartolino